

Article

Tsygankoite, $\text{Mn}_8\text{Tl}_8\text{Hg}_2(\text{Sb}_{21}\text{Pb}_2\text{Tl})_{\Sigma 24}\text{S}_{48}$, a New Sulfosalt from the Vorontsovskoe Gold Deposit, Northern Urals, Russia

Anatoly V. Kasatkin ¹, Emil Makovicky ², Jakub Plášil ^{3,*}, Radek Škoda ⁴ ,
Atali A. Agakhanov ¹, Vladimir Y. Karpenko ¹ and Fabrizio Nestola ⁵

¹ Fersman Mineralogical Museum of Russian Academy of Sciences, Leninsky Prospekt 18-2, Moscow 119071, Russia; anatoly.kasatkin@gmail.com (A.V.K.); atali99@mail.ru (A.A.A.); mineralab@mail.ru (V.Y.K.)

² Department of Geoscience and Resource Management, University of Copenhagen, Østervoldgade 10, DK-1350 Copenhagen, Denmark; emilm@ign.ku.dk

³ Institute of Physics ASCR, v.v.i., Na Slovance 1999/2, Praha 18221, Czech Republic

⁴ Department of Geological Sciences, Faculty of Science, Masaryk University, Kotlářská 2, Brno 61137, Czech Republic; rskoda@sci.muni.cz

⁵ Dipartimento di Geoscienze, Università di Padova, Via Gradenigo 6, Padova I-35131, Italy; fabrizio.nestola@unipd.it

* Correspondence: plasil@fzu.cz; Tel.: +420-775-21-27-57

Received: 2 May 2018; Accepted: 19 May 2018; Published: 21 May 2018



Abstract: Tsygankoite, ideally $\text{Mn}_8\text{Tl}_8\text{Hg}_2(\text{Sb}_{21}\text{Pb}_2\text{Tl})_{\Sigma 24}\text{S}_{48}$, is a new sulfosalt discovered at the Vorontsovskoe gold deposit, Northern Urals, Russia. It occurs as lath-like elongated crystals up to 0.2 mm embedded in calcite–dolomite–clinochlore matrix. The associated minerals also include aktashite, alabandite, arsenopyrite, barite, cinnabar, fluorapatite, orpiment, pyrite, realgar, routhierite, sphalerite, tilasite, and titanite. The new mineral is non-fluorescent, black, and opaque with a metallic lustre and black streak. It is brittle with an uneven fracture and no obvious parting and cleavage. Its Vickers hardness (VHN_{10}) is 144 kg/mm^2 (range 131–167 kg/mm^2) and its calculated density is 5.450 $\text{g}\cdot\text{cm}^{-3}$. In reflected light, tsygankoite is white; between crossed polars it is dark grey to black. It is strongly anisotropic: rotation tints vary from light grey to dark grey to black. Pleochroism and internal reflections are not observed. The chemical composition of tsygankoite (wt %, electron-microprobe data) is: Mn 6.29, Hg 5.42, Tl 26.05, Pb 5.84, As 3.39, Sb 30.89, S 21.87, total 99.75. The empirical formula, calculated on the basis of 90 atoms *pfu*, is: $\text{Mn}_{8.06}\text{Tl}_{8.00}\text{Hg}_{1.90}(\text{Sb}_{17.87}\text{As}_{3.19}\text{Pb}_{1.99}\text{Tl}_{0.97})_{\Sigma 24.02}\text{S}_{48.03}$. Tsygankoite is monoclinic, space group $C2/m$, $a = 21.362(4)$ Å, $b = 3.8579(10)$ Å, $c = 27.135(4)$ Å, $\beta = 106.944(14)^\circ$, $V = 2139.19(17)$ Å³ and $Z = 1$. The five strongest diffraction peaks from X-ray powder pattern (listed as $(d, \text{Å})(I)(hkl)$) are: 3.587(100)(112), 3.353(70)(−114), 3.204(88)(405), 2.841(72)(−513), and 2.786(99)(−514). The crystal structure of tsygankoite was refined from single-crystal X-ray diffraction data to $R = 0.0607$ and consists of an alternation of two thick layer-like arrays, one based on PbS-archetype and the second on SnS-archetype. Tsygankoite has been approved by the IMA-CNMNC under the number 2017-088. It is named for Mikhail V. Tsyganko, a mineral collector from Severouralsk, Northern Urals, Russia, who collected the samples where the new mineral was discovered.

Keywords: tsygankoite; new sulfosalt; thallium; crystal structure; Vorontsovskoe gold deposit

1. Introduction

The actively exploited Vorontsovskoe gold deposit in Northern Urals, Russia, similarly to the famous Lengnabach deposit in Switzerland or Allchar in Macedonia, was found to be the remarkable

source of a particularly interesting Tl–Hg mineralization. Besides several very rare minerals—such as bernardite, chabournéite, christite, dalnegroite, hutchinsonite, imhofite, parapierrotite, picotpaulite, sicherite, vrbaita, etc.—this deposit also yielded three new Tl-bearing minerals already approved by IMA-CNMNC (vorontsovite, ferrovorontsovite, tsygankoite) with few other potentially new species still being under investigation.

In this paper, we describe the new mineral tsygankoite [pronouncing: tsi gan ko ait] while vorontsovite and ferrovorontsovite are described in another paper of the same special issue.

Tsygankoite is named for Mikhail Vladimirovitch Tsyganko (born 25 October 1979), a mineral collector from Severouralsk, Sverdlovskaya Oblast', Northern Urals, Russia. His extensive mineral collection is oriented mostly to the minerals of Northern and Subpolar Urals as well as systematic species served as a base for mineralogical museum "Shtufnoi Kabinet" (Mineral Cabinet), which was founded in 2014 by Mikhail and his friends. Mikhail is the author of the book dedicated to the minerals of Northern Urals [1] where he described in detail the mineralogy of the region and presented the list of all mineral species discovered there so far. The new mineral described here was discovered in the specimens collected by M.V. Tsyganko in June 2015 in the ore stockpile of the Vorontsovskoe deposit. Two other new species from the same deposit (vorontsovite and ferrovorontsovite) were also collected by him.

Both the mineral and its name have been approved by the Commission on New Minerals, Nomenclature and Classification (CNMNC) of the International Mineralogical Association, under the number 2017-088.

The type specimen is deposited in the collections of the Fersman Mineralogical Museum of the Russian Academy of Sciences, Moscow, Russia under the registration number 5018/1.

2. Occurrence

The Vorontsovskoe gold deposit is located 0.5 km west of the settlement of Vorontsovka, approximately 13 km south of the city of Krasnotur'insk, Sverdlovskaya Oblast', Northern Urals, Russia (59°39'5" N, 60°12'56" E). The deposit was discovered in 1985 and is currently operated by Russian mining company Polymetal International PLC for high-grade gold-bearing ore. The ore reserves at 01 January 2017 were estimated at 0.9 million tr.oz of gold and average content of 2.7 g/t. In 2017, the company produced 118,000 tr.oz. of refined gold.

Genesis of the Vorontsovskoe deposit and its main types of ore remains the subject of discussion in Russian geological literature. According to some of the authors, Vorontsovskoe belongs to the Carlin-type deposits [2,3] while others suggest that it is a part of the complex Vorontsovsko–Peschanskaya ore-magmatic system and breccias with orpiment-realgar cement were formed as a result of fluid explosion [4,5].

The geological location of the deposit and composition of its main mineral types of ore is shortly given in companion paper describing two other new Tl-bearing minerals originating from Vorontsovskoe deposit, vorontsovite and ferrovorontsovite, in the same special issue [6].

Similar to vorontsovite and ferrovorontsovite, tsygankoite was found in the ores of the sulfide-carbonate type. They comprise limestone breccias (calcite-dolomite, up to 85% of volume), main silicate minerals (quartz, feldspars, clinocllore, muscovite, up to 10% of volume), accessory minerals, and sulfide-sulfosalt assemblage. Accessory minerals include apatite, arsenic, barite, gold, russellite, titanite, tilasite, and La-analogue of gasparite-(Ce). Apatite forms chemically zoned crystals: they consist mainly of As-Cl-bearing fluorapatite with some compositions corresponding to hydroxylapatite. The As and Cl contents increase from the core to the rim of the crystals up to the appearance of chlorapatite and turneaureite compositions along the edges.

The sulfide-sulfosalt assemblage includes common arsenopyrite, cinnabar, orpiment, pyrite, realgar, sphalerite (including Mn-bearing variety), and rare acanthite, aktashite, alabandine, benavidesite, duranusite, guettardite, jordanite, tennantite, and zinkenite. Thallium mineralization is

represented by dalnegroite and routhierite. Neither vorontsovite nor ferrovorontsovite were found in the same association with tsyankoite.

Tsyankoite should be considered as a very rare mineral. Indeed, its occurrence was so far confirmed in three polished sections only.

3. Physical and Optical Properties

Tsyankoite occurs as black lath-like elongated crystals up to 0.2 mm across embedded in calcite–dolomite–clinochlore matrix. Tsyankoite either forms individual crystals or is partially replaced by alabandite (Figures 1 and 2).

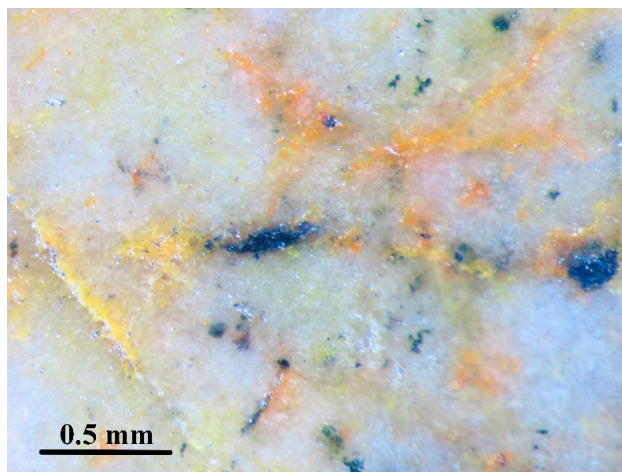


Figure 1. Black elongated grain of tsyankoite with metallic lustre and alabandite (in the center) in white dolomite–calcite matrix along with orpiment (yellow) and native arsenic (black rounded grain on the right). This grain of tsyankoite was extracted from the polished section and used for the structure data collection.

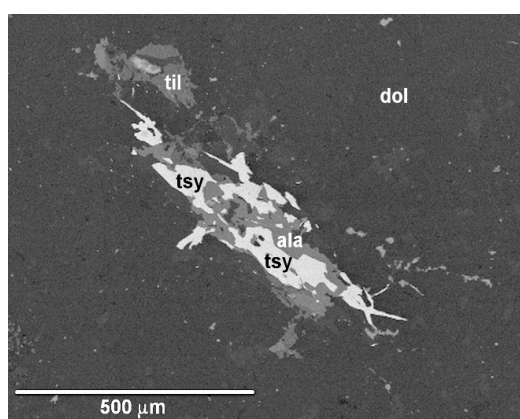


Figure 2. SEM (BSE) image of tsyankoite grain from Figure 1 shows tsyankoite (tsy) being partially replaced by alabandite (ala). Both minerals are associated with tilasite (til) and are embedded in a dolomite–calcite. Polished section.

Tsyankoite is opaque in transmitted light and exhibits metallic luster and black streak. Its tenacity is brittle and fracture—uneven. Cleavage and parting are not observed. It is non-fluorescent. The Vickers hardness (VHN_{10}) is 144 kg/mm^2 (range $131\text{--}167 \text{ kg/mm}^2$) corresponding to a Mohs hardness of ~ 3 . The density could not be measured because of the absence of suitable heavy liquids and paucity of available material. The calculated density based on the empirical formula ($Z = 1$) and unit-cell volume obtained from single-crystal X-ray data is $5.450 \text{ g}\cdot\text{cm}^{-3}$.

In reflected light, tsygankoite is white. It does not show any pleochroism and internal reflections. The bireflectance is very weak, $\Delta R = 4.43\%$ (589 nm). Between crossed polars, the mineral is strongly anisotropic with rotation tints varying from light grey to dark grey to black. Quantitative reflectance measurements were performed in air relative to a WTiC standard by means of a Universal Microspectrophotometer UMSP 50 (Opton-Zeiss, Germany) (Table 1).

Table 1. Reflectance data for tsygankoite.

λ (nm)	R_1 (%)	R_2 (%)
400	33.85	30.53
420	33.64	30.94
440	32.39	30.72
460	32.88	31.56
470	33.16	31.67
480	33.44	31.78
500	33.22	31.71
520	32.84	31.49
540	32.53	31.26
546	32.41	31.11
560	32.26	31.00
580	31.89	30.54
589	31.58	30.18
600	31.51	30.14
620	30.95	29.83
640	30.27	29.10
650	29.83	28.73
660	29.37	28.39
680	28.29	27.58
700	27.41	26.74

Note: Reflectance percentages for the four COM (Commission on Ore Mineralogy) wavelengths are given in bold.

4. Chemical Composition and Chemical Properties

Preliminary chemical analyses using a scanning electron microscope CamScan 4D equipped with INCA Energy microanalyzer (EDS mode, 20 kV, 5 nA and beam diameter 5 μm) showed the presence in tsygankoite of Mn, Tl, Hg, Pb, Sb, As, and S. No other elements with atomic numbers higher than 8 were detected.

Quantitative chemical analyses were conducted in wavelength-dispersive (WDS) mode, using a Cameca SX-100 electron microprobe operated at 25 kV and 20 nA with the beam size of 1 μm . Peak counting times were 20 s for all elements, with one half of the peak time for each background. The following standards, X-ray lines, and analyzing crystals (in parentheses) were used: Mn—Mn metal, $K\alpha$ (LIF); Hg—HgTe, $M\alpha$ (PET); Tl—Tl (Br,I), $M\alpha$ (PET); Pb—PbSe, $M\alpha$ (PET); As—pararammelsbergite, $L\beta$ (TAP); Sb—Sb, $L\beta$ (PET); S—chalcopyrite, $K\alpha$ (PET). Analytical data are given in Table 2 (mean of 7 spot analyses).

Table 2. Chemical data (wt %) for tsygankoite.

Constituent	Mean	Range	SD
Mn	6.29	6.15–6.40	0.11
Hg	5.42	5.31–5.58	0.09
Tl	26.05	25.52–26.53	0.35
Pb	5.84	5.01–6.34	0.59
As	3.39	3.15–3.72	0.21
Sb	30.89	30.32–31.39	0.34
S	21.87	21.40–22.40	0.30
Total	99.75		

Note: SD = standard deviation.

The empirical formula of tsyganokite (based on 90 atoms *pfu*) is: $\text{Mn}_{8.06}\text{Tl}_{8.97}\text{Pb}_{1.98}\text{Hg}_{1.90}\text{Fe}_{0.03}\text{Cu}_{0.02}\text{Ag}_{0.01}\text{Sb}_{17.85}\text{As}_{3.18}\text{S}_{48.00}\text{Se}_{0.01}$. Taking into account the structural data, the formula can be given as: $\text{Mn}_{8.06}\text{Tl}_{8.00}\text{Hg}_{1.90}(\text{Sb}_{17.87}\text{As}_{3.19}\text{Pb}_{1.99}\text{Tl}_{0.97})_{\Sigma 24.02}\text{S}_{48.03}$. The ideal chemical formula is $\text{Mn}_8\text{Tl}_8\text{Hg}_2(\text{Sb}_{21}\text{Pb}_2\text{Tl})_{\Sigma 24}\text{S}_{48}$, which requires Mn 6.11, Tl 25.59, Hg 5.57, Sb 35.56, Pb 5.77, S 21.40, total 100.00 wt %. It is essential that Pb and Tl play an important role in the substitution for $(\text{Sb} + \text{As})^{3+}$ and are necessary for the stabilization of the structure (see below).

Tsyganokite showed to be totally insoluble in acids, aqua regia, and alkalis.

5. X-Ray Crystallography

A small crystal fragment of tsyganokite having $0.032 \text{ mm} \times 0.017 \text{ mm} \times 0.007 \text{ mm}$ across was carefully extracted from the polished section used for EMPA. This grain was used for collection of X-ray data utilizing a Rigaku SuperNova single-crystal diffractometer equipped with the Atlas S2 detector. The instrument is equipped with a Mo micro-focus X-ray tube, working at 50 kV and 0.8 mA (40 W), providing a beam spot of 120 μm . Omega scan mode produced 272 frames in three runs with exposition time of 500 s per frame. Unit-cell parameters were refined from 514 observed reflections. The following data were obtained: tsyganokite is monoclinic, space group $C2/m$, with $a = 21.362(4) \text{ \AA}$, $b = 3.8579(10) \text{ \AA}$, $c = 27.135(4) \text{ \AA}$, $\beta = 106.944(14)^\circ$, $V = 2139.19(17) \text{ \AA}^3$, $Z = 1$.

Due to the lack of suitable material, we present calculated powder pattern of tsyganokite only. The theoretical d_{hkl} and relative intensities were calculated using PowderCell program [7] from the structure model. Data are given in Table 3.

Table 3. Calculated powder X-ray data (d values given in \AA) for tsyganokite (only diffractions with $I_{\text{rel.}} > 5\%$ are listed).

$I_{\text{rel.}}$ (%)	$d_{\text{calc.}}$ (\AA)	h	k	l	$I_{\text{rel.}}$ (%)	$d_{\text{calc.}}$ (\AA)	h	k	l
11	12.98	0	0	2	99	2.786	-5	1	4
29	9.483	-2	0	2	22	2.731	5	1	1
6	7.822	-2	0	3	12	2.711	-2	0	10
27	5.310	-4	0	2	7	2.688	-3	1	7
6	5.109	4	0	0	28	2.604	-5	1	6
11	5.097	-4	0	3	7	2.586	2	0	9
9	4.480	-2	0	6	s6	2.582	1	1	7
16	4.342	4	0	2	8	2.534	-1	1	8
14	4.326	0	0	6	5	2.530	6	0	5
23	3.927	4	0	3	8	2.525	5	1	3
25	3.911	-4	0	6	7	2.490	-5	1	7
38	3.866	-2	0	7	12	2.473	8	0	1
14	3.722	1	1	1	5	2.435	-6	0	10
20	3.708	0	0	7	17	2.368	-7	1	1
100	3.587	1	1	2	23	2.358	-1	1	9
44	3.559	-6	0	2	13	2.328	7	1	0
8	3.543	4	0	4	5	2.275	-6	0	11
25	3.540	-6	0	3	13	2.268	-8	0	9
13	3.511	-6	0	1	7	2.238	1	1	9
12	3.459	-6	0	4	26	2.198	-1	1	10
68	3.391	-2	0	8	13	2.182	3	1	8
70	3.353	-1	1	4	17	2.163	-8	0	10
6	3.327	-6	0	5	12	2.116	-10	0	2
88	3.204	4	0	5	11	2.085	-10	0	1
10	3.161	-6	0	6	9	2.061	-7	1	9
40	3.144	-1	1	5	9	2.054	-1	1	11
7	3.142	3	1	2	13	2.049	5	1	7
6	3.024	-3	1	5	29	2.047	3	1	9
28	3.015	-2	0	9	9	2.021	-9	1	3
45	2.988	3	1	3	9	2.014	-10	0	8

Table 3. Cont.

$I_{rel.}$ (%)	$d_{calc.}$ (Å)	h	k	l	$I_{rel.}$ (%)	$d_{calc.}$ (Å)	h	k	l
7	2.978	−6	0	7	8	1.9608	7	1	5
41	2.910	4	0	6	6	1.9389	5	1	8
13	2.895	6	0	3	53	1.9290	0	2	0
8	2.884	0	0	9	5	1.9241	3	1	10
19	2.863	−5	1	2	37	1.8915	−7	1	11
64	2.858	−3	1	6	7	1.8705	10	0	3
41	2.851	−5	1	1	32	1.8670	9	1	2
72	2.841	−5	1	3	8	1.8649	8	0	7
6	2.821	3	1	4	15	1.8602	2	0	13
60	2.805	5	1	0	15	1.8358	−3	1	13

* values given in bold represent six observed diffractions having the highest relative intensities.

6. Description of Crystal Structure and Discussion

The crystal structure of tsyganokite was refined to $R = 0.0607$ for 957 observed reflections, with criterion $I > 3\sigma(I)$. The crystal structure of tsyganokite was solved from diffraction data using SHELXT [8] and refined using the least-squares algorithm of the Jana2006 program [9]. Data collection and refinement details are listed in Table 4, atom coordinates and displacement parameters along with the bond-valences are listed in Table 5, and selected bond-lengths in Table 6. The CIF file for tsyganokite is available in the Supplementary Materials as file S1.

Table 4. Summary of data collection conditions and refinement parameters for tsyganokite.

Formula	$\text{Mn}_8\text{Tl}_{8.00}\text{Hg}_{2.00}(\text{Sb}_{18.74}\cdot\text{As}_{2.18}\text{Tl}_{1.67}\text{Pb}_{1.44})\Sigma_{24.03}\text{S}_{48}$
Crystal system	monoclinic
Space group	$C2/m$
Unit-cell parameters: a, b, c [Å]	21.362(4), 3.8579(10), 27.135(4)
β [°]	106.944(14)
Unit-cell volume [Å ³]	2139.19(17)
Z	1
Calculated density [g/cm ³]	5.450 (from empirical formula)
Crystal size [mm]	0.032 × 0.017 × 0.007
Diffractometer	Rigaku SuperNova with Atlas S2 CCD
Temperature [K]	295
Radiation, wavelength [Å]	MoK α , 0.71073 (50 kV, 0.8 mA)
θ range for data collection [°]	3.50–27.14
Limiting Miller indices	$h = -26 \rightarrow 26, k = -4 \rightarrow 4, l = -34 \rightarrow 17$
Axis, frame width (°), time per frame (s)	ω , 1.0, 500
Total reflections collected	4686
Unique reflections	2403
Unique observed reflections, criterion	957, [$I > 3\sigma(I)$]
Absorption coefficient [mm ^{−1}], type	33.37; empirical
T_{min}/T_{max}	0.782/1
Data completeness to θ_{max} (%), R_{int}	89.00, 0.105
Structure refinement	Full-matrix least-squares on F^2
No. of param., restraints, constraints	143, 0, 24
R, wR (obs)	0.0607, 0.0943
R, wR (all)	0.1757, 0.1452
GOF obs/all	1.14, 1.04
Weighting scheme, weights	$\sigma, w = 1/(\sigma^2(I) + 0.0001800964I^2)$
Largest diffraction peak and hole (e [−] /Å ³)	7.32 (0.48 Å to Sb6), −7.76

Table 5. Atom positions and displacement parameters (in Å²) for tsyganokite.

Atom	<i>x/a</i>	<i>y/b</i>	<i>z/c</i>	<i>U</i> _{eq}	<i>U</i> ¹¹	<i>U</i> ²²	<i>U</i> ³³	<i>U</i> ¹²	<i>U</i> ¹³	<i>U</i> ²³
Hg1	0.5	1	0.5	0.0243(9)	0.0275(16)	0.0240(17)	0.0240(16)	0	0.0111(13)	0
Tl1	0.61255(10)	−0.5	0.64328(7)	0.0360(8)	0.0448(13)	0.0319(13)	0.0361(12)	0	0.0194(11)	0
Tl2	0.35428(9)	−0.5	0.81477(8)	0.0362(8)	0.0324(12)	0.0313(13)	0.0454(14)	0	0.0122(10)	0
Sb1	0.28499(15)	0	0.45391(11)	0.0259(11)	0.0308(19)	0.0223(19)	0.0231(16)	0	0.0058(15)	0
Sb2	0.33573(19)	0	0.67105(12)	0.0415(14)	0.077(3)	0.019(2)	0.0299(19)	0	0.018(2)	0
Sb3/Pb3	0.4110(2)	−1	0.97915(15)	0.081(2)	0.121(4)	0.049(3)	0.112(4)	0	0.094(3)	0
Sb4/As3	0.53848(18)	0	0.87986(13)	0.0442(17)	0.044(3)	0.057(3)	0.025(2)	0	0.001(2)	0
Sb5/As5	0.67441(18)	0	0.78772(15)	0.0427(17)	0.026(2)	0.050(3)	0.046(3)	0	0.000(2)	0
Sb6/Tl6	0.2295(2)	−1.5	0.92414(15)	0.091(2)	0.173(5)	0.034(2)	0.112(3)	0	0.116(3)	0
Mn1	0.4134(3)	0.5	0.5777(2)	0.023(2)	0.024(4)	0.022(4)	0.022(4)	0	0.006(3)	0
Mn2	0.5162(3)	0.5	0.7581(2)	0.022(2)	0.023(4)	0.026(4)	0.017(3)	0	0.006(3)	0
S1	0.4924(5)	1	0.5836(4)	0.021(4)	0.031(6)	0.023(7)	0.015(6)	0	0.015(5)	0
S2	0.5745(5)	0	0.7221(4)	0.020(4)	0.025(6)	0.020(6)	0.015(5)	0	0.007(5)	0
S3	0.4225(5)	0.5	0.6753(4)	0.024(4)	0.018(6)	0.029(7)	0.021(6)	0	−0.002(5)	0
S4	0.3232(5)	0	0.5780(4)	0.020(4)	0.033(7)	0.018(6)	0.010(5)	0	0.007(5)	0
S5	0.3698(5)	0.5	0.4759(4)	0.023(4)	0.019(6)	0.022(7)	0.033(7)	0	0.012(6)	0
S6	0.2750(5)	0	0.3625(4)	0.024(4)	0.033(7)	0.021(7)	0.018(6)	0	0.005(6)	0
S7	0.4610(6)	0	0.7970(4)	0.026(4)	0.036(7)	0.020(7)	0.021(6)	0	0.005(6)	0
S8	0.7220(6)	−0.5	0.7473(4)	0.037(5)	0.025(7)	0.053(9)	0.031(7)	0	0.004(6)	0
S9	0.6079(7)	0.5	0.8437(4)	0.044(5)	0.049(9)	0.053(10)	0.019(6)	0	−0.006(7)	0
S10	0.3047(7)	−1	0.8969(5)	0.047(6)	0.045(9)	0.058(11)	0.033(7)	0	0.001(7)	0
S11	0.3311(8)	−1.5	1.0129(5)	0.062(6)	0.096(13)	0.029(9)	0.035(8)	0	−0.021(8)	0
S12	0.4678(9)	−0.5	0.9152(6)	0.080(8)	0.104(14)	0.016(8)	0.079(11)	0	−0.037(11)	0

Refined occupancies: Sb3 site = 0.64(2)Sb/0.36(2)Pb; Sb4 site = 0.77(3)Sb/0.23(3)As; Sb5 site = 0.68(3)Sb/0.32(3)As; Sb6 site = 0.59(2)Sb/0.41(2)Tl.

Table 6. Selected interatomic distances (Å) in tsyganokite.

Hg1–S1	2.321(11) (2×)	Sb3–S11	2.896(14) (2×)
Tl1–S1	3.242(8) (2×)	Sb4–S7	2.373(10)
Tl1–S2	3.158(10) (2×)	Sb4–S9	2.781(11) (2×)
Tl1–S5	3.363(12)	Sb4–S12	2.786(15) (2×)
Tl1–S6	3.119(9) (2×)	Sb5–S2	2.347(10) (2×)
Tl1–S8	3.096(10) (2×)	Sb5–S8	2.570(9) (2×)
Tl2–S7	3.129(11) (2×)	Sb6–S10	2.745(12) (2×)
Tl2–S8	3.470(9) (2×)	Sb6–S11	2.733(13)
Tl2–S10	3.344(13) (2×)	Mn1–S1	2.573(8) (2×)
Tl2–S12	3.075(15)	Mn1–S3	2.598(12)
Sb1–S4	2.940(8) (2×)	Mn1–S4	2.728(9) (2×)
Sb1–S5	2.594(7) (2×)	Mn1–S5	2.645(11)
Sb1–S6	2.427(11)	Mn2–S2	2.633(10) (2×)
Sb2–S3	2.665(8) (2×)	Mn2–S3	2.536(10)
Sb2–S4	2.459(11)	Mn2–S7	2.636(10) (2×)
Sb2–S6	2.981(8) (2×)	Mn2–S9	2.565(12)
Sb3–S10	2.679(13)		

The crystal structure of tsyganokite contains 11 independent cation sites (four of which are mixed sites which were refined with one set of coordinates each) and 12 distinct sulfur sites. It consists of an alternation of two thick layer-like arrays; both are typical for sulfosalt structures.

The array based on PbS-archetype (i.e., with a PbS-like topology) contains a Hg site with a typical bond scheme, a Tl site, the octahedrally coordinated Mn1 site, and two pure Sb sites, labeled Sb1 and Sb2. The alternating array, based on the SnS-archetype (an array with a more pronounced steric role of lone electron pairs), with a general bond scheme represented by that observed in SnS [10], contains four distinct Sb sites, all of which statistically mix with either heavier cations (refined as Pb or Tl component) or with arsenic. Embedded in this array is a thallium site (refined as “Tl3”), and a Mn²⁺ site, this being apical to the second array. Interesting is the close spatial relationship of large Tl⁺ and small Mn²⁺ polyhedra in the former array and along its contact with the latter array.

The PbS-like portions represent a sequence of interconnected rods, four (100)_{PbS} planes thick, ideally three polyhedra broad but heavily overlapped (rod-based sulfosalt structures were defined in

Makovicky [11]). The contact/overlap portions of two adjacent rods are formed by the coordination octahedron of Hg, surrounded by two Mn octahedra and two bicapped trigonal coordination prisms of Tl; paired columns of Sb coordination pyramids form the cores of rods, with a lone electron space in between the pyramidal pairs (Figure 3).

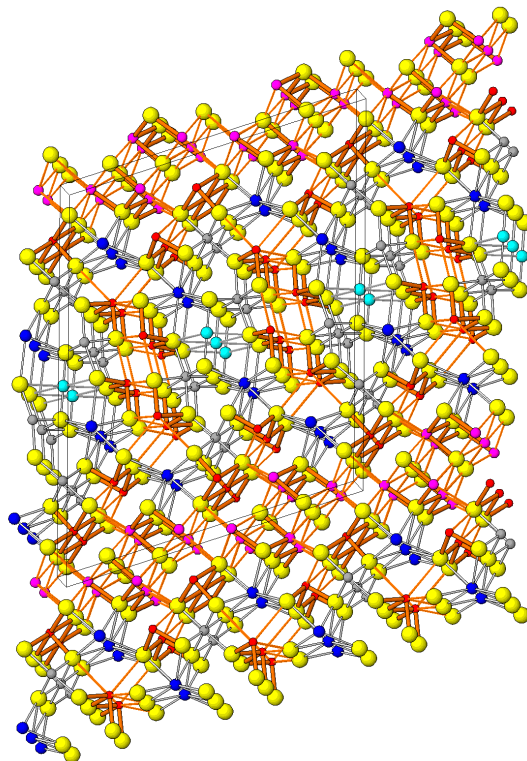


Figure 3. Crystal structure of tsgankoite in projection onto (010). Yellow spheres: S; blue spheres: Tl; turquoise: Hg; red: Sb and (Sb,As); mauve: (Sb,Pb,Tl); grey: Mn. Short, strong Sb–S bonds: thick orange lines, longer distances: thin lines. Remaining cation–anion connections: bonds and distances defining the complete coordination polyhedron. The *c* direction is upward oriented; inclined slightly.

The contact of rods differs from those which were known when Makovicky [11] classified rod-based sulfosalt structures. In the present case, the rods are interconnected via three atomic $(100)_{\text{PbS}}$ planes (Figure 3), whereas at that time, only rod interconnections/overlaps via one or two such planes were known. The only hitherto published situation close to the here-described one occurs in the PbS-archetype layers of the crystal structure of rouxelite $\text{Cu}_2\text{HgPb}_{22}\text{Sb}_{28}\text{S}_{64}(\text{O,S})_2$ [12], in which two adjacent rod-like bulges periodically occur, interconnected and amalgamated via octahedrally coordinated Hg site.

The general orientation of the PbS-based layers is (510) regarding a pseudo-tetragonal subcell which can be defined from Figure 3, and it is (522) regarding a cubic PbS-like subcell which can be defined as an alternative in this layer (Figure 4).

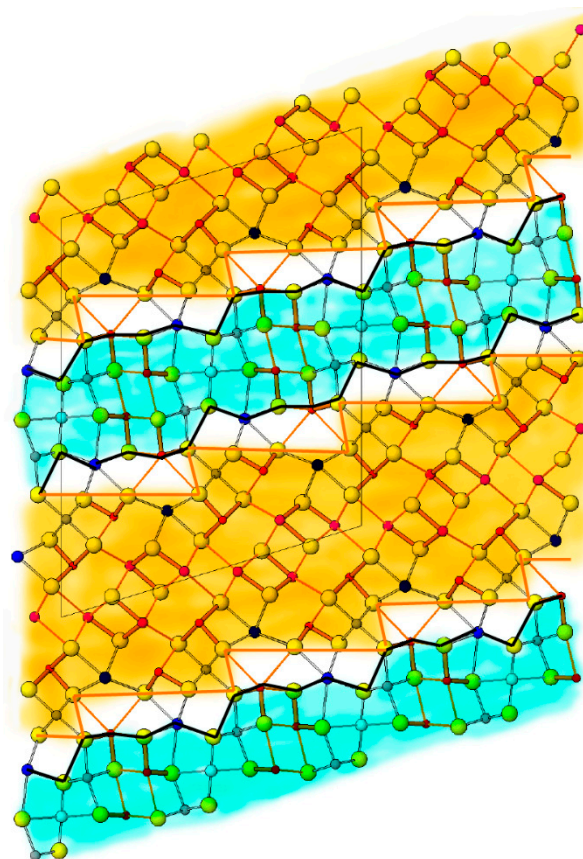


Figure 4. The crystal structure of tsyganokite in terms of mercury containing layers with PbS topology (blue) alternating with Sb-rich layers with SnS-like topology (orange). For atom species see Figure 3. Unit cell edges outlined in black solid line.

The layer based on the SnS-archetype represents a step-like cut-out of an SnS-like, antimony-based sulfide slab, limited by the overall $(410)_{\text{SnS}}$ planes (Figure 4). It consists of a set of double-ribbons which are diagonal to the overall orientation of this slab (Figure 3), tightly bonded by Sb–S bonds in the ribbon interior, and contain planar interspaces which house lone electron pairs, spaced between them. In subsurface portions of double-ribbons, one site is occupied by thallium (Tl3), whereas the step tips are formed by an octahedron of Mn (Mn2). The distribution of shorter and longer bonds in the central portions of this layer differs from that in SnS and is made possible only by lengthening of cation–sulfur bonds due to the partial substitutions of Sb by (Pb,Tl), as described in detail further below. The Sb3–Sb6 distance is 4.196 Å. The complicated match of the two-layer arrays proceeds via Mn octahedra, followed by a space for lone electron pairs of Sb from the PbS-like layer, Tl from the SnS-like layer, and a trigonal coordination prism of Tl (Tl2).

The flattened coordination octahedron of Hg consists of a linear configuration S1–Hg–S1 (bond length 2.320 Å) accompanied by four long Hg–S distances of 3.290 Å. This corresponds well with such values from cinnabar, HgS [13], which are 2.368 Å (2×), 3.094 Å (2×), and 3.287 Å (2×). Another example is the structure of balkanite, $\text{Cu}_9\text{Ag}_5\text{HgS}_8$ [14], with the Hg–S distances equal to 2.366 Å (2×) and 3.300 Å (4×). The thallium polyhedra have trigonal prismatic distances between 3.120 and 3.240 Å, and between 3.129 and 3.470 Å, respectively for Tl2 and Tl3, with capping distances 3.096 and 3.363 Å, and 3.075 Å, in the same order. This suggests pure thallium sites.

Manganese octahedra are fairly regular, especially the Mn2 site (Mn–S distance from 2.536 to 2.636 Å). The asymmetrically positioned Mn1 site is somewhat less regular (from 2.539 to 2.728 Å). This compares very well with the Mn octahedra in MnSb_2S_4 : the orthorhombic modification [15] has

octahedral Mn–S distances between 2.537 and 2.692 Å, the monoclinic modification [16] has two sites with ranges 2.546–2.643 Å and 2.611–2.614 Å, respectively.

The antimony sites Sb1 and Sb2 in the rod-like structure portions have the typical signature of Sb^{3+} , with the Sb–S distances to the vertex of the coordination pyramid equal to 2.427 Å and 2.460 Å, respectively, opposed by 3.225 Å and 3.621 plus 3.676 Å in the same sequence. In the pyramidal base, the distances and their opposites are 2.594 Å vs. 2.940 Å, and 2.654 Å vs. 2.982 Å (each twice) in the above order.

According to the refinement, Sb3 and Sb6 contain 0.36 “Pb” and 0.41 “Tl”, respectively, these being mixture of Pb and, also presumably, Tl. The more marginal sites Sb4 and Sb5 contain 0.23 As and 0.32 As, respectively. These mixed sites show correspondingly altered bond distances: Sb3 has the “Sb”–S distance to the pyramidal vertex equal to 2.680 Å and the bond scheme in the pyramidal base much more equalized—2.895 Å opposed by 3.071 Å. Sb 6 has the same values equal to 2.732 Å, 2.746 Å, and 3.099 Å. The calculations below show that the substituting atoms are a mixture of Pb and Tl.

The substitution by arsenic manifests itself by the vertex-oriented Sb–S distances, which are equal to 2.372 Å for Sb4 and 2.348 Å for Sb5, which can be compared with such distances for Sb1 and Sb2 (above). The in-base distances reveal a complete or at least a partial positional disorder, 2.781 vs. 2.786 Å for Sb4 and 2.571 vs. 3.050 Å for the marginal position Sb5.

Comparison of the empirical chemical formula and the refinement results is as follows: from chemical analyses, the unit cell contains $\text{Mn}_{8.06}\text{Tl}_{8.97}\text{Pb}_{1.98}\text{Hg}_{1.90}\text{Fe}_{0.03}\text{Cu}_{0.02}\text{Ag}_{0.01}\text{Sb}_{17.85}\text{As}_{3.18}\text{S}_{48.00}\text{Se}_{0.01}$. Whereas the structure schematically shows $\text{Mn}_8\text{Tl}_8\text{Hg}_2(\text{Sb,As})_{12}(\text{Sb,Pb,Tl})_{12}\text{S}_{48}$. This suggests a spectrum of substitutions and substituted sites (all values that follow are the *apfu* values). Let’s consider the mercury site to be fully occupied and to contain 2 Hg. Thallium fully occupies two sites, 8 Tl *pfu*, which leaves 0.97 Tl for combination with Pb in substituting for Sb and As in the central portions of the SnS-like slabs. The EMPA suggests that there should be about three heavy atoms (Tl + 2Pb) at the central Sb sites; from the structure it gives 1.67 Tl and 1.44 Pb, thus only a slight excess. Structure determination gives 2.18 As, in insufficient agreement with chemically ascertained 3.18 As per formula unit. Both differences can be caused either by slightly distinct chemistry of the grain used for EMPA and the fragment of that grain used for SCXRD or are due to less perfect resolution of Sb/As and Sb/Pb + Sb/Tl distribution among the Sb sites. To conclude, the (Sb + As + Pb) value of 23.01 *apfu* from the chemical analysis plus remaining 0.97 Tl yields 23.98 atoms, very close to the expected sum of 24 *apfu* for “Sb” sites.

The structure of tsyankoite is unique among minerals. This is the first mineral having Mn, Tl, tsyankoite fits best in Subdivision 2.HD (Sulfosalts of SnS-archetype with Tl).

Supplementary Materials: The following are available online at www.mdpi.com/2075-163X/8/5/218/s1. Supplementary file S1: Crystallographic information file for tsyankoite.

Author Contributions: A.V.K. found the new mineral in polished sections of the studied samples; E.M. and J.P. performed the X-ray structural investigations; R.Š. and A.V.K. conducted the electron-microprobe analyses; A.A.A. and V.Y.K. determined the optical, physical, and chemical properties; A.V.K., E.M., J.P. and F.N. wrote the paper.

Acknowledgments: This research was supported by the project no. LO1603 under the Ministry of Education, Youth and Sports National sustainability program I of the Czech Republic to J.P.

Conflicts of Interest: The authors declare no conflict of interest.

References

1. Tsyganko, M.V. *Kamennyi Uzor Zemli Vagranskoi. Mineraly Severouralskogo Rayona (Stone Design of Vagranskaya Earth. Minerals of Northern Urals); “Kvist”*: Yekaterinburg, Russia, 2015; 120p. (In Russian)
2. Sazonov, V.N.; Murzin, V.V.; Grigor’ev, N.A. Vorontsovsk gold deposit: An example of carlin-type mineralization in the Urals, Russia. *Geol. Ore Depos.* **1998**, *40*, 139–151.
3. Murzin, V.V.; Naumov, E.A.; Azovskova, O.B.; Varlamov, D.A.; Rovnushkin, M.Y.; Pirajno, F. The Vorontsovskoe Au-Hg-As ore deposit (Northern Urals, Russia): Geological setting, ore mineralogy, geochemistry, geochronology and genetic model. *Ore Geol. Rev.* **2017**, *85*, 271–298. [[CrossRef](#)]

4. Minina, O.V. The Auerbahovskiy complex ore-magmatic system of the Middle Ural. *Nativ. Geol.* **1994**, *7*, 17–23. (In Russian)
5. Stepanov, S.Y.; Sharpenok, L.N.; Antonov, A.V. Fluid-exposive breccias of the Vorontsovskoe gold deposit (The North Urals). *Zapiski RMO* **2017**, *1*, 29–43. (In Russian)
6. Kasatkin, A.V.; Nestola, F.; Agakhanov, A.A.; Škoda, R.; Karpenko, V.Y.; Tsyganko, M.V.; Plášil, J. Vorontsovite, $(\text{Hg}_5\text{Cu})_{\Sigma 6}\text{TlAs}_4\text{S}_{12}$, and ferrovorontsovite, $(\text{Fe}_5\text{Cu})_{\Sigma 6}\text{TlAs}_4\text{S}_{12}$: The Tl- and Tl-Fe-analogues of Galkhaite from the Vorontsovskoe gold deposit, Northern Urals, Russia. *Minerals* **2018**, *8*, 185. [[CrossRef](#)]
7. Kraus, W.; Nolze, G. POWDER CELL—A program for the representation and manipulation of crystal structures and calculation of the resulting X-ray powder patterns. *J. Appl. Cryst.* **1996**, *29*, 301–303. [[CrossRef](#)]
8. Sheldrick, G.M. SHELXT—Integrated space-group and crystal-structure determination. *Acta Crystallogr. Sect. A* **2015**, *71*, 3–8. [[CrossRef](#)] [[PubMed](#)]
9. Petříček, V.; Dušek, M.; Palatinus, L. Crystallographic computing system Jana2006: General features. *Z. Kristallogr.* **2014**, *229*, 345–352. [[CrossRef](#)]
10. Makovicky, E. The building principles and classification of sulphosalts based on the SnS archetype. *Fortschr. Mineral.* **1985**, *63*, 45–89.
11. Makovicky, E. Rod-based sulphosalt structures derived from the SnS and PbS archetypes. *Eur. J. Mineral.* **1993**, *5*, 545–591. [[CrossRef](#)]
12. Orlandi, P.; Meerschaut, A.; Moëlo, Y.; Palvadeau, P.; Léone, P. Lead-antimony sulfosalts from Tuscany (Italy). VIII. Rouxelite, $\text{Cu}_2\text{HgPb}_{22}\text{Sb}_{28}\text{S}_{64}(\text{O},\text{S})_2$, a new sulfosalt from Buca della Vena mine, Apuan Alps: definition and crystal structure. *Can. Mineral.* **2005**, *43*, 919–933. [[CrossRef](#)]
13. Auvray, P.; Genet, F. Affinement de la structure cristalline du cinabre, alpha HgS. *Bull. Soc. Fr. Min. Cristallogr.* **1973**, *96*, 218–219.
14. Biagioni, C.; Bindi, L. Ordered distribution of Cu and Ag in the crystal structure of balkanite, $\text{Cu}_9\text{Ag}_5\text{HgS}_8$. *Eur. J. Mineral.* **2017**, *29*, 279–285. [[CrossRef](#)]
15. Bente, K.; Edenharter, A. Roentgenographische Strukturanalyse von MnSb_2S_4 und Strukturverfeinerung von Berthierit, FeSb_2S_4 . *Z. Kristallogr.* **1989**, *186*, 31–33.
16. Pfitzner, A.; Kurowski, D. A new modification of MnSb_2S_4 crystallizing in the HgBi_2S_4 structure type. *Z. Kristallogr.* **2000**, *215*, 373–376. [[CrossRef](#)]



© 2018 by the authors. Licensee MDPI, Basel, Switzerland. This article is an open access article distributed under the terms and conditions of the Creative Commons Attribution (CC BY) license (<http://creativecommons.org/licenses/by/4.0/>).